

KVzap: Fast, Adaptive, and Faithful KV Cache Pruning

Simon Jégou* Maximilian Jeblick

 NVIDIA/KVzap  NVIDIA/kvpress

Abstract. Growing context lengths in transformer-based language models have made the key-value (KV) cache a critical inference bottleneck. While many KV cache pruning methods have been proposed, they have not yet been adopted in major inference engines due to speed–accuracy trade-offs. We introduce KVzap, a fast, input-adaptive approximation of KVzip that works in both prefilling and decoding. On Qwen3-8B, Llama-3.1-8B-Instruct, and Qwen3-32B across long-context and reasoning tasks, KVzap achieves 2–4× KV cache compression with negligible accuracy loss and achieves state-of-the-art performance on the  KVpress Leaderboard. Code and models are available at  NVIDIA/kvpress.

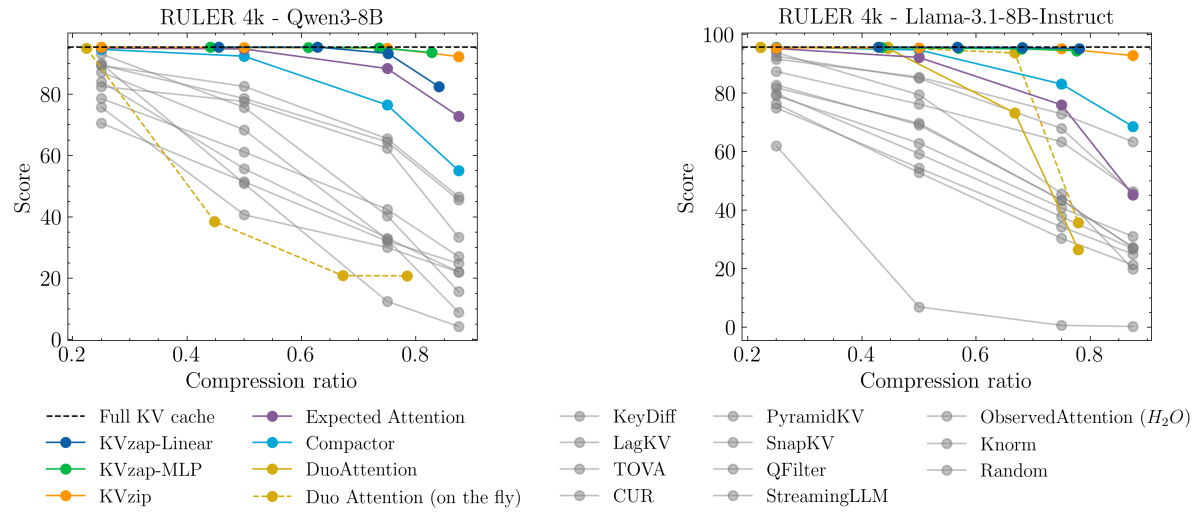


Figure 1 |  KVpress Leaderboard for Qwen3-8B (left) and Llama-3.1-8B-Instruct (right) comparing different KV cache pruning methods. The plots compare the accuracy on the RULER 4k dataset (Hsieh et al., 2024) (y-axis) against the KV cache compression ratio (x-axis). KVzap achieves state-of-the-art performance on both models, matching KVzip (Kim et al., 2025) — which it approximates — while outperforming 15 other methods, including Expected Attention (Devoto et al., 2025), Duo Attention (Xiao et al., 2024), and Compactor (Chari & Durme, 2025).

1. Introduction

In transformer attention (Vaswani et al., 2017), each input token produces a set of key-value (KV) vector pairs that are stored in a cache and reused during autoregressive generation. The KV cache has shape $(2, L, H, T, D)$, where L is the number of layers, H the number of heads, T the sequence length, and D the key/value dimension. For example, in bfloat16 precision, the KV cache for a vanilla transformer like Llama1-65B (Touvron et al., 2023) ($L = 80$, $H = 64$, $D = 128$) requires 335 GB of memory at $T = 128k$. As sequence lengths grow to tens or hundreds of thousands of tokens, the KV cache becomes a dominant bottleneck for efficient LLM inference (Fu, 2024), increasing GPU peak memory usage and time to first token while reducing decoding throughput.

*Main contributor. Contact: sjegou@nvidia.com

Over the years, several architectural modifications have targeted specific axes of the KV cache to reduce its size. Along the H -axis, Grouped Query Attention (GQA, (Ainslie et al., 2023)) shares keys and values across multiple queries, yielding KV cache compression factors of $4\times$ (Llama3, (Llama Team, 2024)), $12\times$ (GLM 4.5, (GLM-4.5 Team, 2025)), and up to $16\times$ (Qwen3-235B-A22B, (Qwen Team, 2025)). Along the D -axis, DeepSeek V2 (DeepSeek-AI, 2024) introduces Multi-head Latent Attention (MLA) to perform a low-rank decomposition of keys and values, equivalent to a $4H/9$ compression. Along the L -axis, recent hybrid models interleave attention layers with sliding window attention ($2\times$ compression for GPT-OSS-120B (OpenAI, 2025), $6\times$ for Gemma3 (Gemma Team, 2025)) or state space models ($8\times$ compression for Jamba (Lieber et al., 2024), $4\times$ compression for Kimi-Linear (Kimi Team, 2025), $4.8\times$ for Nemotron3 Nano (NVIDIA, 2025)).

Notably, no widely adopted architectural change compresses the KV cache along the T -axis. Sparse attention mechanisms, such as DSA in DeepSeek V3.2 (DeepSeek-AI, 2025), retrieve only the most relevant KV pairs at each decoding step and can improve throughput, but they do not reduce the KV cache memory size.

Most attempts at KV cache compression on the T -axis rely on *ad-hoc* pruning methods. Sparse attention is motivated by the idea that, within a head, attending to all past KV pairs is unnecessary for the *next* decoding step; KV cache pruning goes further and assumes that some KV pairs will never be attended to *at all*. Just as a reader does not pay equal attention to every word when understanding a sentence, not all tokens are equally important, and some need not occupy HL slots in KV cache memory. By retaining only KV pairs that are likely to be accessed, pruning methods can substantially reduce memory while preserving the information needed for faithful generation.

Pioneered by H_2O (Zhang et al., 2023), the Awesome-KV-Cache-Compression repository now lists dozens of KV cache pruning methods, with 20+ implemented in  NVIDIA/kvpress. While these methods validate the pruning intuition—e.g., KVzip (Kim et al., 2025) can reach $4\times$ compression with no accuracy loss on some tasks—none have been integrated into major inference engines such as vLLM (Kwon et al., 2023b), SGLang (Zheng et al., 2023), or TRT-LLM (NVIDIA, 2023). In retrospect, each solution fails to meet at least one of the following criteria:

- **Criterion 1: Fast and lightweight.** The pruning overhead must be negligible.
- **Criterion 2: Phase-agnostic.** The method must apply to both prefilling (long context) and decoding (reasoning tasks).
- **Criterion 3: Optimization-friendly.** The method must be compatible with kernels like FlashAttention2 (Dao, 2023) or PagedAttention (Kwon et al., 2023a)
- **Criterion 4: Faithful.** The method should cause minimal accuracy degradation on any task.

In this work, we introduce KVzap, a fast approximation of KVzip. Our contributions are the following:

- We enhance the KVzip scoring with a normalization term inspired by (Devoto et al., 2025), creating **KVzip+**.
- We demonstrate that KVzip+ scores can be approximated by a lightweight surrogate model trained on top of the model’s hidden states.
- We introduce **KVzap**, a new KV cache pruning technique which applies these surrogate models to the hidden states to prune KV pairs below a fixed threshold τ .

2. Method

Summary: In each transformer layer, KVzap applies a lightweight model to the input hidden states to predict importance scores and discards KV pairs whose score falls below a threshold τ . The KVzap model is trained to approximate the scoring policy of an improved KVzip variant (Kim et al., 2025).

2.1. KVzip

KVzip (Kim et al., 2025) currently stands as the state-of-the-art KV cache pruning method on the  KVpress Leaderboard. While it reaches up to $4\times$ compression with minimal accuracy loss, it has major

limitations that hinder adoption. First, it requires prefilling on an extended prompt twice as long as the input, making it prohibitively slow. Second, it cannot be used during decoding, which makes it unsuitable for reasoning tasks that generate thousands of tokens.

KVzip relies on a copy-and-paste pretext task to score the most important KV pairs. Given an input context `user: <prompt>` whose KV cache is to be compressed, it starts by building an extended prompt:

```
user: <prompt>
Repeat the previous context exactly.
assistant: <prompt>
```

Then, for each head, the KV pair at position i in the original `<prompt>` is scored as the maximum attention weight over the repeated `<prompt>` (and over heads in a group when GQA is used):

$$s_i = \max_{j \in \text{<prompt>}} a_{ji} \quad (1)$$

Finally, the lowest-scoring KV pairs across heads and layers are removed. The intuition is that if, in a given head, the model pays little attention to position i in the original `<prompt>` when repeating `<prompt>`, then the KV pair at i carries little information and can be discarded.

2.2. KVzip+

We enhance KVzip scoring by incorporating the analysis from (Devoto et al., 2025). For a given transformer head at decoding step j , the hidden-state update is:

$$\mathbf{h}_j^{out} = \mathbf{h}_j + \sum_{i \leq j} a_{ji} W_O \mathbf{v}_i \quad (2)$$

where \mathbf{h}_j is the input hidden state, \mathbf{h}_j^{out} the output hidden state, W_O the output projection matrix, and \mathbf{v}_i the value vector. The term $a_{ji} W_O \mathbf{v}_i$ represents token i 's contribution to the residual stream \mathbf{h}_j . We incorporate this normalization into Eq. (1) to define the KVzip+ score:

$$s_i^+ = \max_{j \in \text{<prompt>}} a_{ji} \frac{\|W_O \mathbf{v}_i\|}{\|\mathbf{h}_j\|} \quad (3)$$

2.3. KVzap

To address KVzip's limitations, we train a per-layer surrogate—either a linear layer or a two-layer MLP—to predict H scores $\log(s^+)$ directly from the input hidden states \mathbf{h} (we use log-space to match the exponential nature of softmax attention). The model acts independently at each sequence position t : it maps $\mathbf{h}_t \in \mathbb{R}^{D_h}$ to scores in \mathbb{R}^H , where D_h is the hidden dimension and H is the number of KV heads. Because it uses only one or two matrix multiplications and depends only on hidden states, KVzap is computationally efficient (see Appendix B) and can be applied during decoding.

For training, we curate 1.2M pairs $(\mathbf{h}, \log(s^+))$ per KV head, sampled from  Nemotron-Pretraining-Dataset-sample. The dataset is diverse, covering English, multilingual, code, and mathematical text.

Another key difference lies in the eviction policy. Whereas KVzip enforces a fixed budget (e.g., keeping exactly 50% of KV pairs), KVzap uses thresholding, discarding KV pairs whose predicted score falls below a fixed threshold τ . Higher thresholds yield higher compression ratios. This makes KVzap input-adaptive: it dynamically adapts the compression rate based on the prompt information density, retaining more tokens for complex inputs and fewer for redundant ones.

Finally, to preserve local context, we keep a sliding window of the most recent $w = 128$ tokens, following StreamingLLM (Xiao et al., 2023). The full procedure is detailed in Algorithm 1.

```

def compress(hidden_states, keys, values, kvzap_model, threshold, window=128):
    scores = kvzap_model(hidden_states)
    scores[..., -window:] = float("inf")
    indices = torch.where(scores >= threshold)
    return keys[indices], values[indices]

```

Algorithm 1 | PyTorch pseudocode for KV cache pruning using KVzap during prefilling. Decoding is similar but needs a score buffer to enforce the sliding window

3. Experiments

All experiments were run on Qwen3-8B, Llama-3.1-8B-Instruct, and Qwen3-32B and are fully reproducible via  NVIDIA/kvpress. Trained models are available in the  NVIDIA/KVzap collection, and full evaluation logs are provided in  KVzap predictions.

3.1. KVzap training

To generate training pairs $(\mathbf{h}, \log(s^+))$, we leveraged  Nemotron-Pretraining-Dataset-sample. The dataset contains 27k prompts split into 9 subsets (common crawl, multilingual, math, code, etc.). We filtered prompts to a length of 750–1,250 tokens to minimize the impact of sequence lengths on attention weights and then selected up to 500 prompts per subset for training and 5 for validation, resulting in roughly 2.4k prompts. We then randomly sampled 500 tokens per prompt to obtain 1.2M training pairs (per head), with 23k held out for validation.

For each KV head, we trained two types of surrogate models to predict $\log(s^+)$ from the hidden state \mathbf{h} : a linear model (**KVzap-Linear**) and a two-layer MLP (**KVzap-MLP**). The input dimension matches the model hidden size ($D_h = 4096$ or 5120), and the output dimension is the number of KV heads ($H = 8$). For MLPs, we used one hidden layer with width $D_h/8$ (512 or 640), followed by a GELU activation. In practice, KVzap-Linear and KVzap-MLP consist of a list of L PyTorch modules (Paszke et al., 2019), with input size (T, D_h) and output size (T, H) .

We report the average Squared Pearson correlation (R^2) over the HL KV heads on the validation set in Table 1. Both surrogates reach R^2 in the 0.60–0.80 range, showing that the expensive KVzip+ score can be approximated from hidden states. Across all models, KVzap-MLP consistently outperforms KVzap-Linear. A more detailed analysis is provided in Appendix A.

Table 1 | Average R^2 between KVzip+ scores and KVzap predictions on the validation set.

Model	Linear	MLP
Qwen3-8B	0.671	0.711
Llama-3.1-8B-Instruct	0.743	0.772
Qwen3-32B	0.629	0.668

3.2. Compute and memory overhead

KVzap adds negligible overhead: across all models, its relative compute cost is bounded by 1.1% for KVzap-MLP and 0.02% for KVzap-Linear when considering linear projections *only* (Table 3 in Appendix B). The relative memory overhead matches these bounds, and in long-context regimes the quadratic attention cost dominates, making KVzap’s overhead negligible. Finally, during decoding—which is strictly memory-bandwidth bound—KVzap’s additional FLOPs effectively utilize idle GPU cycles that would otherwise be stalled by KV cache retrieval (Recasens et al., 2025).

3.3. Prefilling and decoding tasks

KV cache pruning is most impactful for tasks involving thousands of tokens, during prefilling (long inputs) or decoding (long outputs). To assess KVzap across these regimes, we evaluate KVzap-Linear and KVzap-MLP on two long-context benchmarks—RULER (Hsieh et al., 2024) ($n = 6500$) and LongBench (Bai et al., 2024) ($n = 4750$)—and one reasoning benchmark, AIME25 (Zhang & Math-AI, 2025) ($n = 30$).

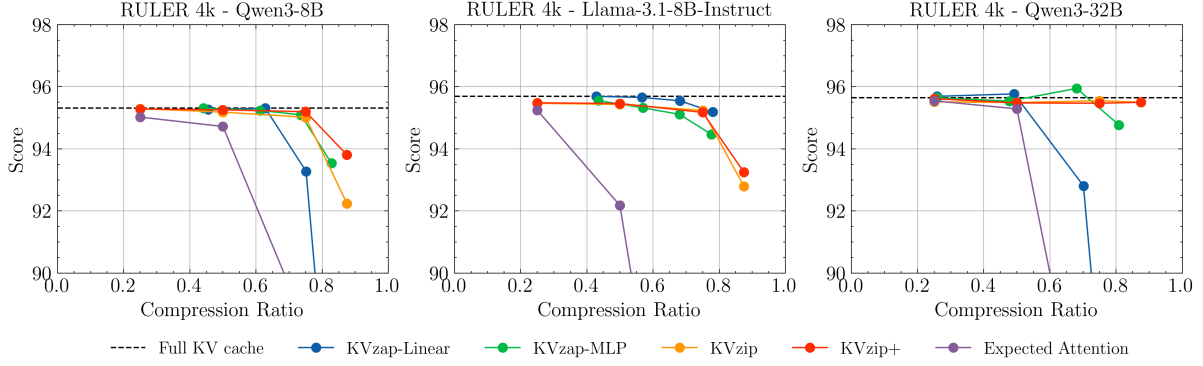


Figure 2 | **RULER 4k** results for Qwen3-8B (left), Llama-3.1-8B-Instruct (middle), and Qwen3-32B (right). Zoomed-in view (y-axis range [90, 100]) of the high-performance region from Figure 1. KVzap surrogates perform comparably to—and sometimes exceed—the KVzip+ oracle they approximate.

Experimental Setup We evaluate KVzap using thresholds $\tau \in \{-6, -5, -4, -3\}$ for Qwen3-8B and Qwen3-32B, and $\tau \in \{-9, -8, -7, -6\}$ for Llama-3.1-8B-Instruct. For RULER and LongBench, we used greedy decoding and disabled reasoning; for AIME25, we evaluated Qwen3-8B and Qwen3-32B models with reasoning and sampling parameters recommended in the Qwen3 model card (temperature = 0.6, top- p = 0.95, top- k = 20). In all experiments, KV cache compression was applied after the attention operation.

3.4. RULER

RULER (Hsieh et al., 2024) evaluates long-context capabilities across four task categories—retrieval, multi-hop tracing, aggregation, and question answering—over 13 subsets with sequence lengths ranging from 4k to 128k.

On RULER 4k, KVzap achieves state-of-the-art results for both Qwen3-8B and Llama-3.1-8B-Instruct (Figure 1), significantly outperforming 15 concurrent KV cache pruning methods.

We provide a magnified view in Figure 2, comparing KVzap variants against KVzip, KVzip+, and Expected Attention (Devoto et al., 2025). A few trends emerge: (1) KVzip+ consistently matches or exceeds KVzip, validating our normalization; (2) KVzap maintains perfect accuracy up to 3–4 \times compression; (3) For Qwen models, KVzap-MLP outperforms KVzap-Linear, which degrades sharply at high compression; (4) surprisingly, KVzap-Linear excels on Llama-3.1-8B-Instruct despite lower R^2 than KVzap-MLP and even outperforms the KVzip+ oracle it approximates.

3.5. LongBench

LongBench (Bai et al., 2024) evaluates long-context capabilities across six task categories—single-document QA, multi-document QA, summarization, few-shot learning, synthetic tasks, and code completion—spanning 21 subsets in English and Chinese. We report the average performance across subsets in Figure 3.

Mirroring the main RULER results, (1) KVzip+ consistently matches or outperforms KVzip, and (2) KVzap models maintain near-perfect accuracy up to 2–3 \times compression. Notably, the same thresholds τ yield lower compression ratios, likely due to data characteristics: RULER samples are synthetic and repetitive, whereas LongBench consists mostly of real-world data with higher information density.

At first glance, Expected Attention (Devoto et al., 2025) appears to surpass the full KV cache baseline for Qwen3-8B and Llama-3.1-8B-Instruct at lower compression ratios. A closer look reveals this is largely driven by outlier accuracies on the TREC subset (see Figure 12, 13 and 14), and that Expected Attention degrades on several subsets where KVzap stays close to the full KV cache baseline. Higher TREC accuracy at high compression may be explained by the over-prompting phenomenon (Tang et al., 2025): in a few-shot learning task like TREC, adding more examples can counter-intuitively reduce accuracy.

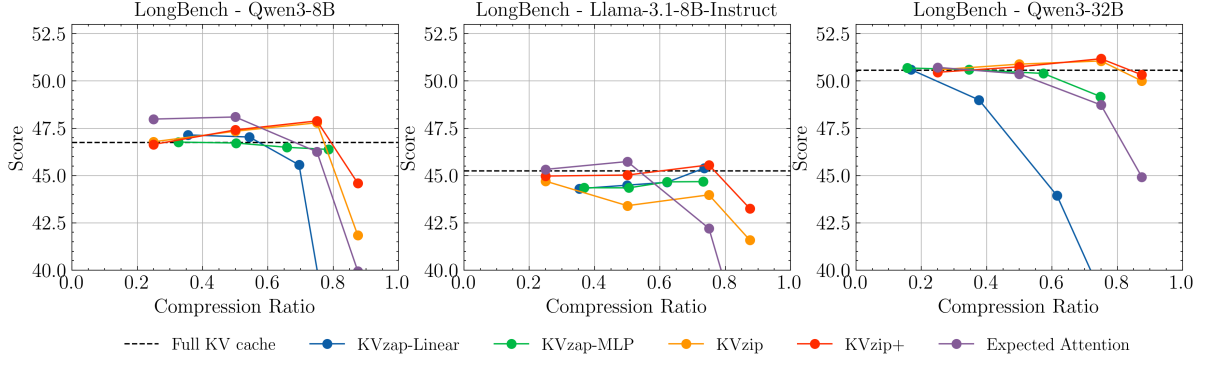


Figure 3 | **LongBench results** for Qwen3-8B (left), Llama-3.1-8B-Instruct (middle), and Qwen3-32B (right). KVzap models again maintain accuracy close to the full KV cache baseline. The elevated scores for Expected Attention are primarily driven by outliers in TREC, one of the 21 subsets of LongBench; see Figure 12 for results excluding TREC.

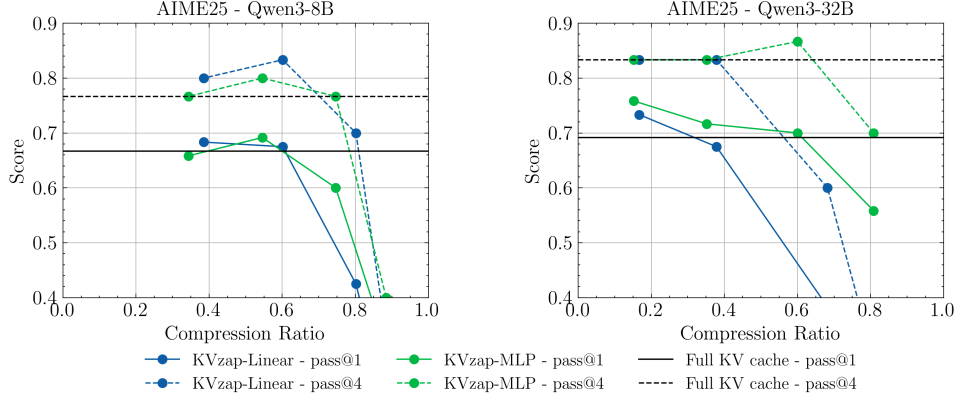


Figure 4 | **AIME25 Reasoning Performance.** Comparison of pass@1 (solid lines) and pass@4 (dashed lines) accuracy for Qwen3-8B (left) and Qwen3-32B (right). KVzap-MLP maintains robust performance even when discarding over 50% of the KV cache.

The generally low accuracy on most LongBench subsets, combined with their small size (typically $n = 200$), leads to high variance, making results harder to interpret conclusively.

3.6. AIME25

The AIME25 benchmark (Zhang & Math-AI, 2025) consists of 30 Olympiad-level, integer-answer problems from the 2025 American Invitational Mathematics Examination. We evaluated KVzap with 4 rollouts per question, a generation limit of 32k tokens, and we report average pass@1 and pass@4 in Figure 4. KVzap-MLP preserves reasoning accuracy even at compression ratios exceeding 2 \times .

3.7. Adaptive compression

Figures 2, 3, and 4 show that the maximum compression that does not degrade accuracy is task-dependent (e.g., higher on RULER and lower on LongBench). KVzap’s thresholding captures this automatically: the same threshold τ translates into different compression ratios across benchmarks.

Table 2 reports the best KVzap configuration (Linear/MLP and τ) per model. Overall, KVzap achieves 2.7–3.5 \times average KV cache compression while maintaining accuracy across model scales and tasks.

Table 2 | Performance of KVzap across models and datasets. Arrows (\rightarrow) show the change from full to compressed KV cache. Values in parentheses indicate the KV cache compression ratio (removed fraction). For each model, we report the best KVzap configuration (Linear/MLP and threshold τ).

	Qwen3-8B	Llama-3.1-8B	Qwen3-32B
KVzap model	MLP	Linear	MLP
Parameters	76M	1.1M	210M
Threshold	$\tau = -4$	$\tau = -7$	$\tau = -4$
RULER 4k	95.32 \rightarrow 95.09 (0.74)	95.69 \rightarrow 95.55 (0.68)	95.65 \rightarrow 95.95 (0.68)
RULER 16k	92.99 \rightarrow 92.78 (0.72)	93.42 \rightarrow 93.29 (0.70)	95.19 \rightarrow 94.96 (0.65)
LongBench	46.74 \rightarrow 46.49 (0.66)	45.25 \rightarrow 44.65 (0.62)	50.56 \rightarrow 50.40 (0.57)
AIME25 (pass@4)	0.77 \rightarrow 0.77 (0.75)	—	0.83 \rightarrow 0.87 (0.60)
Average compression ratio	0.72 (3.5 \times)	0.67 (3.0 \times)	0.63 (2.7 \times)

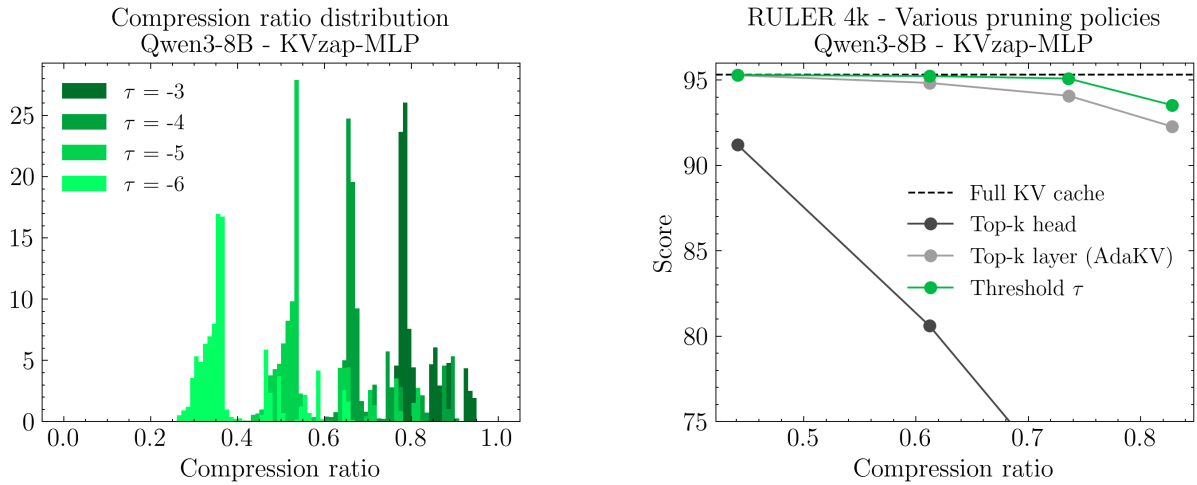


Figure 5 | Distribution of compression ratios for Qwen3-8B and KVzap-MLP on RULER 4k, LongBench, and AIME25 (left), and comparison to an alternative pruning method (right).

3.8. Ablations

Threshold-based pruning KVzap uses score thresholding rather than fixed top- k selection, allowing the compression rate to adapt to prompt complexity. Figure 5 (left) highlights this adaptability, showing up to 20% variation across prompts. As shown in Figure 5 (right), thresholding outperforms fixed-ratio top- k selection, whether per-head or per-layer (AdaKV, (Feng et al., 2025)).

Sliding Window We analyze the impact of sliding-window size w on LongBench-LCC with Qwen3-8B, KVzap-MLP, and $\tau = -4$. Without a local window ($w = 0$), accuracy drops to 28.37% because the input hidden states do not explicitly encode position information. Enforcing $w = 128$ restores performance to 62.51%, while increasing to $w = 512$ yields no additional gain (62.37%).

4. Discussion

Across multiple models (Qwen3-8B, Llama-3.1-8B-Instruct, Qwen3-32B) and benchmarks (RULER, LongBench, AIME25), we show that KVzap achieves 2–4 \times KV cache compression with negligible accuracy loss. Its design—a lightweight linear or MLP model applied to hidden states—is computationally efficient and easy to integrate. Still, limitations and future directions remain.

Scope and Generalization First, while results on a 32B model are encouraging, further validation is needed on larger open-source models (e.g., GLM 4.7 (GLM-4.5 Team, 2025), Qwen3-235B-A22B (Qwen Team, 2025)) and architectures with sparse attention (e.g., DeepSeek V3.2, (DeepSeek-AI, 2025)). Evaluation could also be extended to more reasoning benchmarks, agentic tasks, and short-context knowledge tasks.

Ad-hoc vs. End-to-End Training Second, KVzap is not training-free, and like most KV cache pruning methods, it is a post-hoc addition. In the long run, end-to-end integration often prevails in deep learning, much as Multi-Token Prediction (Gloeckle et al., 2024) is superseding ad-hoc speculative decoding techniques such as Medusa (Cai et al., 2024). Although still rare, end-to-end pruning objectives like DMS (Łańcucki et al., 2025) exist and may eventually yield better performance. Nonetheless, KVzap provides further evidence that LLMs do not fully exploit the KV cache and that unused KV pairs can be easily identified from hidden states.

Implementation Challenges Third, turning compression into wall-clock speedups and GPU memory savings requires careful engineering and was not explored here. KVzap introduces non-uniform cache lengths across heads, requiring PagedAttention kernels (Kwon et al., 2023a) that handle variable-length blocks. Prior work such as DMS (Łańcucki et al., 2025), Compactor (Chari & Durme, 2025), AdaKV (Feng et al., 2025), have shown this is feasible, but kernel optimization remains non-trivial. Since KVzap relies only on hidden states, pruning could also be applied before attention to directly accelerate prefilling.

Conclusion Despite these challenges, we believe KVzap’s combination of simplicity, high compression ratios, and robust performance across tasks and models makes it a prime candidate for production deployment, potentially bridging the gap between academic pruning research and real-world inference engines.

Acknowledgments

We thank Alessio Devoto for his careful reading of the manuscript and for providing detailed and constructive feedback.

References

Joshua Ainslie, James Lee-Thorp, Michiel de Jong, Yury Zemlyanskiy, Federico Lebrón, and Sumit Sanghai. Gqa: Training generalized multi-query transformer models from multi-head checkpoints, 2023. URL <https://arxiv.org/abs/2305.13245>.

Yushi Bai, Xin Lv, Jiajie Zhang, Hongchang Lyu, Jiankai Tang, Zhidian Huang, Zhengxiao Du, Xiao Liu, Aohan Zeng, Lei Hou, Yuxiao Dong, Jie Tang, and Juanzi Li. Longbench: A bilingual, multitask benchmark for long context understanding, 2024. URL <https://arxiv.org/abs/2308.14508>.

Tianle Cai, Yuhong Li, Zhengyang Geng, Hongwu Peng, Jason D. Lee, Deming Chen, and Tri Dao. Medusa: Simple llm inference acceleration framework with multiple decoding heads, 2024. URL <https://arxiv.org/abs/2401.10774>.

Vivek Chari and Benjamin Van Durme. Compactor: Calibrated query-agnostic kv cache compression with approximate leverage scores, 2025. URL <https://arxiv.org/abs/2507.08143>.

Tri Dao. Flashattention-2: Faster attention with better parallelism and work partitioning. *arXiv preprint arXiv:2307.08691*, 2023. URL <https://arxiv.org/abs/2307.08691>.

DeepSeek-AI. Deepseek-v2: A strong, economical, and efficient mixture-of-experts language model. *arXiv preprint arXiv:2405.04434*, 2024. URL <https://arxiv.org/abs/2405.04434>.

DeepSeek-AI. Deepseek-v3.2: Pushing the frontier of open large language models. *arXiv preprint arXiv:2512.02556*, 2025. URL <https://arxiv.org/abs/2512.02556>.

Alessio Devoto, Maximilian Jeblick, and Simon Jégou. Expected attention: Kv cache compression by estimating attention from future queries distribution. *arXiv preprint arXiv:2510.00636*, 2025. URL <https://arxiv.org/abs/2510.00636>.

Yuan Feng, Junlin Lv, Yukun Cao, Xike Xie, and S. Kevin Zhou. Ada-kv: Optimizing kv cache eviction by adaptive budget allocation for efficient llm inference, 2025. URL <https://arxiv.org/abs/2407.11550>.

Yao Fu. Challenges in deploying long-context transformers: A theoretical peak performance analysis, 2024. URL <https://arxiv.org/abs/2405.08944>.

Gemma Team. Gemma 3 technical report, 2025. URL <https://arxiv.org/abs/2503.19786>.

GLM-4.5 Team. Glm-4.5: Agentic, reasoning, and coding (arc) foundation models. *arXiv preprint arXiv:2508.06471*, 2025. URL <https://arxiv.org/abs/2508.06471>.

Fabian Gloeckle, Badr Youbi Idrissi, Baptiste Rozière, David Lopez-Paz, and Gabriel Synnaeve. Better & faster large language models via multi-token prediction, 2024. URL <https://arxiv.org/abs/2404.19737>.

Cheng-Ping Hsieh, Simeng Sun, Samuel Kriman, Shantanu Acharya, Dima Rekesh, Fei Jia, Yang Zhang, and Boris Ginsburg. Ruler: What's the real context size of your long-context language models?, 2024. URL <https://arxiv.org/abs/2404.06654>.

Jang-Hyun Kim, Jinuk Kim, Sangwoo Kwon, Jae W. Lee, Sangdoo Yun, and Hyun Oh Song. Kvzip: Query-agnostic kv cache compression with context reconstruction. *arXiv preprint arXiv:2505.23416*, 2025. URL <https://arxiv.org/abs/2505.23416>.

Kimi Team. Kimi linear: An expressive, efficient attention architecture, 2025. URL <https://arxiv.org/abs/2510.26692>.

Woosuk Kwon, Zhuohan Li, Siyuan Zhuang, Ying Sheng, Lianmin Zheng, Cody Hao Yu, Joseph E. Gonzalez, Hao Zhang, and Ion Stoica. Efficient memory management for large language model serving with pagedattention, 2023a. URL <https://arxiv.org/abs/2309.06180>.

Woosuk Kwon, Zhuohan Yu, Guo Li, Zhiqiang Fan, Zhenhua Chen, Heming Zhang, Cheng-Yu Hsieh, William Ellis, HyoukJoong Yang, Kurt Keutzer, Joseph E. Gonzalez, and Ion Stoica. vllm: Easy, fast, and cheap llm serving with paged attention. *arXiv preprint arXiv:2309.06180*, 2023b. URL <https://arxiv.org/abs/2309.06180>.

Opher Lieber, Barak Lenz, Hofit Bata, Gal Cohen, Jhonathan Osin, Itay Dalmedigos, Erez Safahi, Shaked Meirom, Yonatan Belinkov, Shai Shalev-Shwartz, Omri Abend, Raz Alon, Tomer Asida, Amir Bergman, Roman Glzman, Michael Gokhman, Avashalom Manevich, Nir Ratner, Noam Rozen, Erez Shwartz, Mor Zusman, and Yoav Shoham. Jamba: A hybrid transformer-mamba language model, 2024. URL <https://arxiv.org/abs/2403.19887>.

Llama Team. The llama 3 herd of models, 2024. URL <https://arxiv.org/abs/2407.21783>.

NVIDIA. Tensorrt-llm. <https://github.com/NVIDIA/TensorRT-LLM>, 2023. Open-source library for optimized LLM inference.

NVIDIA. Nvidia nemotron 3: Efficient and open intelligence, 2025. URL <https://arxiv.org/abs/2512.20856>.

OpenAI. Gpt-oss: Open-weight models from openai. <https://github.com/openai/gpt-oss>, 2025. Accessed: 2025-12-10.

Adam Paszke, Sam Gross, Francisco Massa, Adam Lerer, James Bradbury, Gregory Chanan, Trevor Killeen, Zeming Lin, Natalia Gimelshein, Luca Antiga, Alban Desmaison, Andreas Köpf, Edward Yang, Zach DeVito, Martin Raison, Alykhan Tejani, Sasank Chilamkurthy, Benoit Steiner, Lu Fang, Junjie Bai, and Soumith Chintala. Pytorch: An imperative style, high-performance deep learning library, 2019. URL <https://arxiv.org/abs/1912.01703>.

F. Pedregosa, G. Varoquaux, A. Gramfort, V. Michel, B. Thirion, O. Grisel, M. Blondel, P. Prettenhofer, R. Weiss, V. Dubourg, J. Vanderplas, A. Passos, D. Cournapeau, M. Brucher, M. Perrot, and E. Duchesnay. Scikit-learn: Machine learning in Python. *Journal of Machine Learning Research*, 12: 2825–2830, 2011.

Qwen Team. Qwen3 technical report, 2025. URL <https://arxiv.org/abs/2505.09388>.

Pol G. Recasens, Ferran Agullo, Yue Zhu, Chen Wang, Eun Kyung Lee, Olivier Tardieu, Jordi Torres, and Josep Ll. Berral. Mind the memory gap: Unveiling gpu bottlenecks in large-batch llm inference, 2025. URL <https://arxiv.org/abs/2503.08311>.

Yongjian Tang, Doruk Tuncel, Christian Koerner, and Thomas Runkler. The few-shot dilemma: Over-prompting large language models, 2025. URL <https://arxiv.org/abs/2509.13196>.

Marian Tietz, Thomas J. Fan, Daniel Nouri, Benjamin Bossan, and skorch Developers. *skorch: A scikit-learn compatible neural network library that wraps PyTorch*, July 2017. URL <https://skorch.readthedocs.io/en/stable/>.

Hugo Touvron, Thibaut Lavril, Gautier Izacard, Xavier Martinet, Marie-Anne Lachaux, Timothée Lacroix, Baptiste Rozière, Naman Goyal, Eric Hambro, Faisal Azhar, Aurélien Rodriguez, Armand Joulin, Edouard Grave, and Guillaume Lample. LLaMA: Open and efficient foundation language models, 2023. URL <https://arxiv.org/abs/2302.13971>.

Ashish Vaswani, Noam Shazeer, Niki Parmar, Jakob Uszkoreit, Llion Jones, Aidan N. Gomez, Łukasz Kaiser, and Illia Polosukhin. Attention is all you need. *Proceedings of the 31st International Conference on Neural Information Processing Systems*, 2017.

Guangxuan Xiao, Jiannan Tian, Huan Bao, Peng Yan, Shangguang Di, and Tao Xie. Streamingllm: Efficient streaming inference of large language models with attention sinks. *arXiv preprint arXiv:2309.17453*, 2023. URL <https://arxiv.org/abs/2309.17453>.

Guangxuan Xiao, Jiaming Tang, Jingwei Zuo, Junxian Guo, Shang Yang, Haotian Tang, Yao Fu, and Song Han. Duoattention: Efficient long-context llm inference with retrieval and streaming heads, 2024. URL <https://arxiv.org/abs/2410.10819>.

Yifan Zhang and Team Math-AI. American invitational mathematics examination (aime) 2025, 2025.

Zhenyu Zhang, Ying Sheng, Tianyi Zhou, Tianlong Chen, Lianmin Zheng, Ruisi Cai, Zhao Song, Yuandong Tian, Christopher Ré, Clark Barrett, Zhangyang Wang, and Beidi Chen. H₂o: Heavy-hitter oracle for efficient generative inference of large language models. *arXiv preprint arXiv:2306.14048*, 2023. URL <https://arxiv.org/abs/2306.14048>.

Lianmin Zheng, Liangsheng Yin, Zhiqiang Xie, Jeff Huang, Chuyue Sun, Cody Hao Yu, Shiyi Cao, Christos Kozyrakis, Ion Stoica, Joseph E. Gonzalez, Clark Barrett, and Ying Sheng. Sqlang: Efficient execution of structured language model programs. *arXiv preprint arXiv:2312.07104*, 2023. URL <https://arxiv.org/abs/2312.07104>.

Adrian Łaniczcki, Konrad Staniszewski, Piotr Nawrot, and Edoardo M. Ponti. Inference-time hyper-scaling with kv cache compression, 2025. URL <https://arxiv.org/abs/2506.05345>.

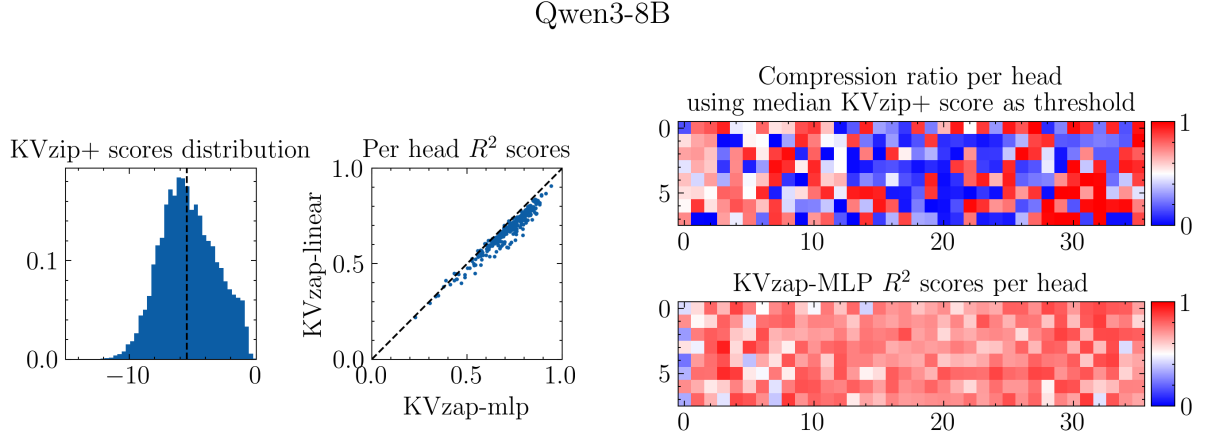


Figure 6 | Detailed KVzap evaluation analysis for Qwen3-8B. **Left:** Distribution of KVzip+ scores computed on the 23k validation pairs. **Middle:** Correlation between the R^2 performance of KVzap-MLP (x-axis) and KVzap-Linear (y-axis) for each head. **Upper Right:** Fraction of KV pairs falling below the median KVzip+ score. **Lower Right:** Heatmap of R^2 scores for KVzap-MLP across all heads.

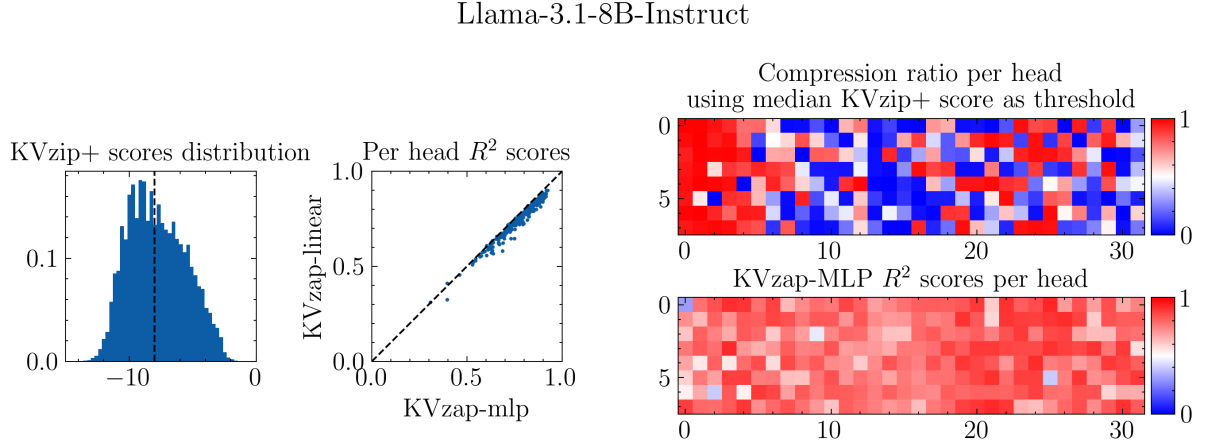


Figure 7 | Detailed KVzap evaluation analysis for Llama-3.1-8B-Instruct. **Left:** Distribution of KVzip+ scores computed on the 23k validation pairs. **Middle:** Correlation between the R^2 performance of KVzap-MLP (x-axis) and KVzap-Linear (y-axis) for each head. **Upper Right:** Fraction of KV pairs falling below the median KVzip+ score. **Lower Right:** Heatmap of R^2 scores for KVzap-MLP across all heads.

A. KVzap model training

We report detailed distributions of KVzip+ and R^2 scores in Figures 6 (Qwen3-8B), 7 (Llama-3.1-8B-Instruct), and 8 (Qwen3-32B).

The Llama-3.1-8B-Instruct score distribution is significantly lower than for Qwen3-8B and Qwen3-32B, motivating lower pruning thresholds in our experiments. Across all models, KVzap-MLP consistently achieves higher R^2 than KVzap-Linear. Both surrogates perform worse in the first transformer layer, suggesting that KVzip+ scores are harder to infer from token embeddings alone. Predicting scores directly from keys and values (\mathbf{k}, \mathbf{v}) instead of hidden states \mathbf{h} resulted in strictly lower R^2 . We also acknowledge a potential train-test distribution shift as KVzap is trained on prompts limited to 1,250 tokens.

We trained KVzap-Linear using scikit-learn (Pedregosa et al., 2011) and KVzap-MLP using skorch (Tietz et al., 2017). Future work could further improve accuracy through better data selection and

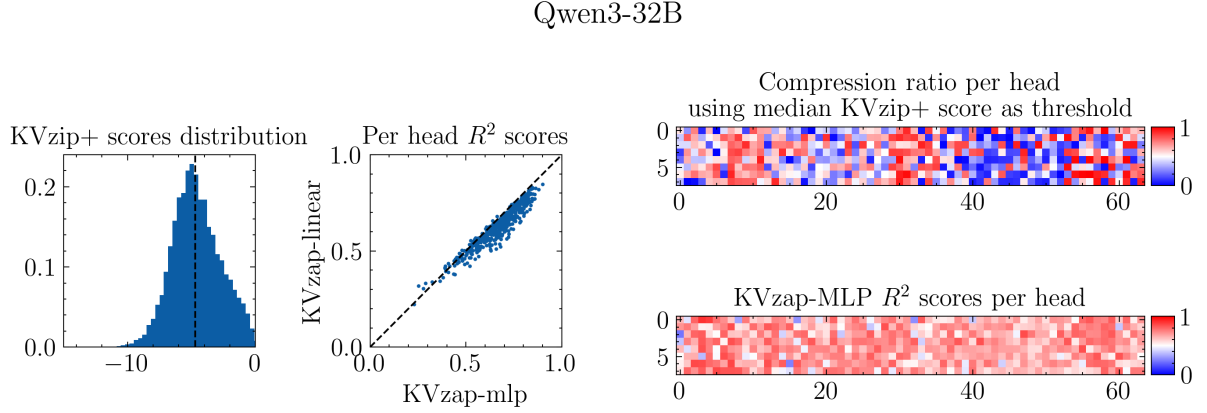


Figure 8 | Detailed KVzap evaluation analysis for Qwen3-32B. **Left:** Distribution of KVzip+ scores computed on the 23k validation pairs. **Middle:** Correlation between the R^2 performance of KVzap-MLP (x-axis) and KVzap-Linear (y-axis) for each head. **Upper Right:** Fraction of KV pairs falling below the median KVzip+ score. **Lower Right:** Heatmap of R^2 scores for KVzap-MLP across all heads.

hyperparameter tuning.

B. KVzap compute and memory overhead

We analyze the compute overhead introduced by KVzap within a single transformer decoder layer, relative to the cost of all linear projections in the layer: the attention projection matrices (W_Q, W_K, W_V, W_O) and the feed-forward network (FFN). We ignore the quadratic attention matrix multiplication and nonlinearities, yielding a conservative upper bound on the relative compute cost.

Assuming a GQA setting with H_Q query heads, H key-value heads, head dimension D , hidden dimension D_h , and a SwiGLU FFN intermediate dimension D_{int} , the FLOPs from linear projections are:

$$C = C_{\text{attn}} + C_{\text{ffn}} = 4D_h(H_QD + HD) + 6D_hD_{\text{int}}, \quad (4)$$

We compare against KVzap-MLP, consisting of two linear layers $W_1 \in \mathbb{R}^{D_h \times D_h/8}$ and $W_2 \in \mathbb{R}^{D_h/8 \times H}$:

$$C_{\text{KVzap-MLP}} = 2 \left(D_h \cdot \frac{D_h}{8} \right) + 2 \left(\frac{D_h}{8} \cdot H \right) = \frac{D_h}{4} (D_h + H) \quad (5)$$

and KVzap-Linear, consisting of a single projection from D_h to H :

$$C_{\text{KVzap-Linear}} = 2D_hH \quad (6)$$

Model	H_Q	H	D	D_h	D_{int}	$\frac{C_{\text{KVzap-MLP}}}{C}$	$\frac{C_{\text{KVzap-Linear}}}{C}$
Qwen3-8B	32	8	128	4096	12288	1.09%	0.02%
Llama-3.1-8B-Instruct	32	8	128	4096	14336	0.96%	0.02%
Qwen3-32B	64	8	128	5120	25600	0.67%	0.01%

Table 3 | Relative compute overhead of KVzap compared to a single transformer layer, considering only linear projections.

Table 3 reports the resulting relative compute overhead for Qwen3-8B, Llama-3.1-8B-Instruct, and Qwen3-32B, showing a maximum overhead of 1.1% for KVzap-MLP and 0.02% for KVzap-Linear. In long-context regimes, the quadratic cost of attention dominates the overall complexity, making this overhead effectively negligible.

Table 4 | AIME25 number of correct answers ($n = 30$) for Qwen3-8B and Qwen3-32B across four rollouts. KVzap-Linear with $\tau = -3$ achieved 96% compression for Qwen3-8B and 93% for Qwen3-32B, explaining the zero scores.

Method	Threshold (τ)	Qwen3-8B	Qwen3-32B
Full KV Cache	-	18, 20, 21, 21	19, 20, 22, 22
KVzap-Linear	-3	0, 0, 0, 0	0, 0, 0, 0
	-4	10, 12, 13, 16	11, 11, 11, 13
	-5	17, 21, 21, 22	17, 21, 21, 22
	-6	19, 20, 21, 22	21, 22, 22, 23
KVzap-MLP	-3	7, 9, 11, 11	16, 16, 17, 18
	-4	16, 17, 19, 20	20, 20, 22, 22
	-5	20, 20, 21, 22	20, 21, 22, 23
	-6	18, 20, 20, 21	22, 22, 23, 24

The relative memory overhead (ignoring biases) matches the compute overhead, as the factor of two introduced in FLOPs counting cancels out in the ratio.

Overall, KVzap’s additional parameters introduce no meaningful memory or compute overhead.

C. Detailed benchmark results

RULER Figures 9–11 provide per-subset results for RULER 4k (Qwen3-8B, Llama-3.1-8B-Instruct, Qwen3-32B).

LongBench Figures 13–15 provide per-subset LongBench results (Qwen3-8B, Llama-3.1-8B-Instruct, Qwen3-32B). We also report the average score excluding TREC in Figure 12.

AIME25 We report results for each of the four rollouts of AIME25 in Table 4.

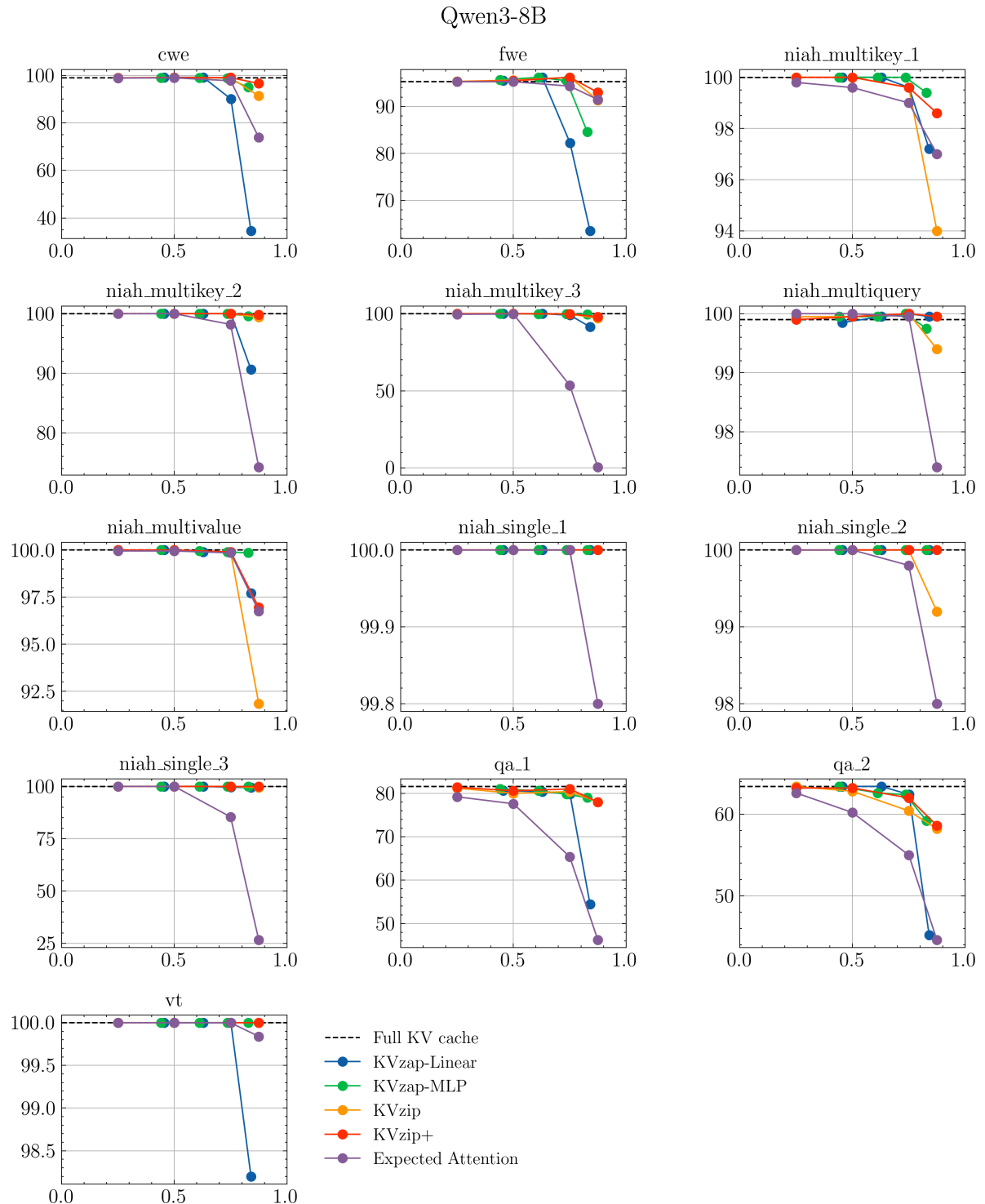


Figure 9 | RULER 4k results for Qwen3-8B on each of the 13 subsets

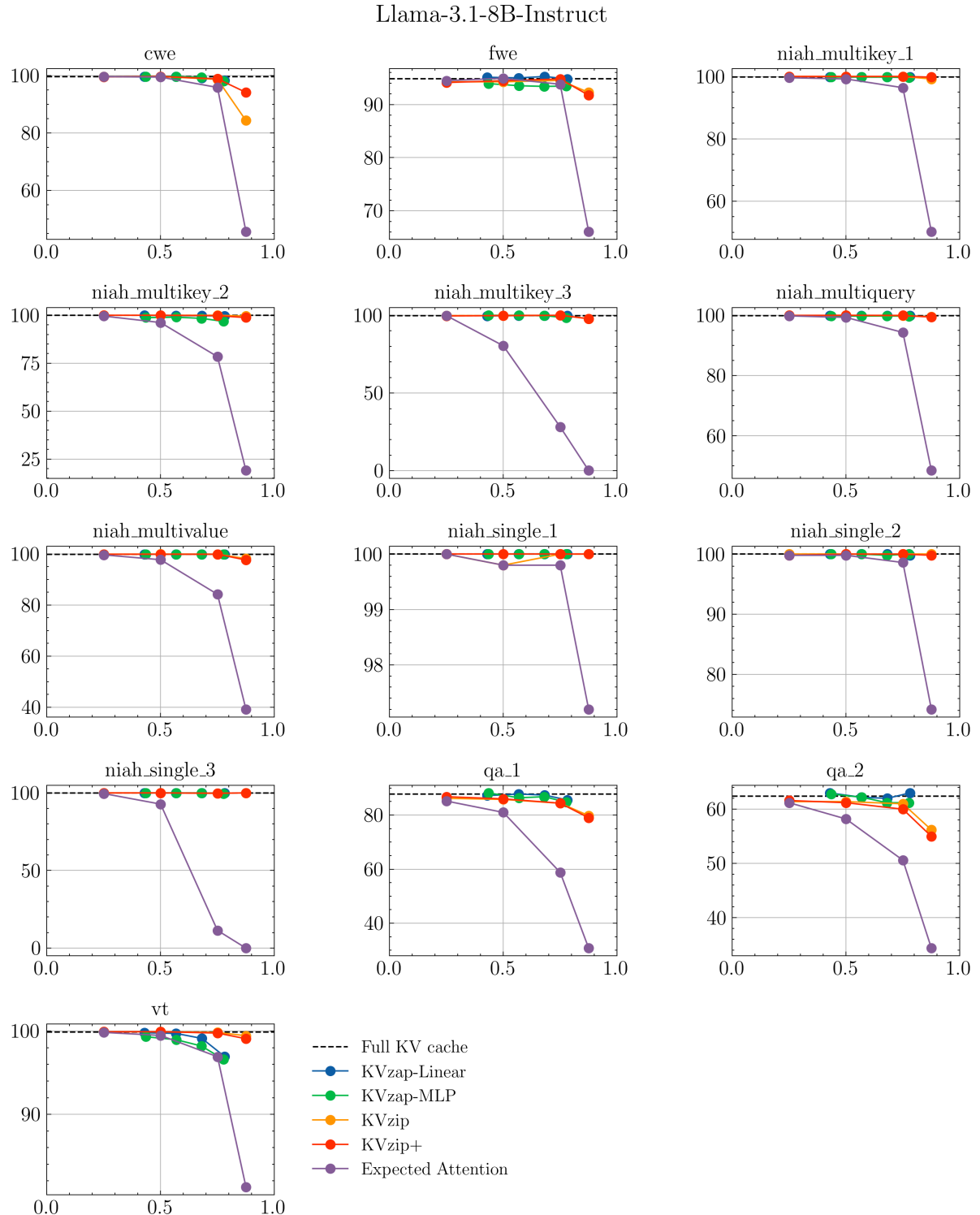


Figure 10 | RULER 4k results for Llama-3.1-8B-Instruct on each of the 13 subsets

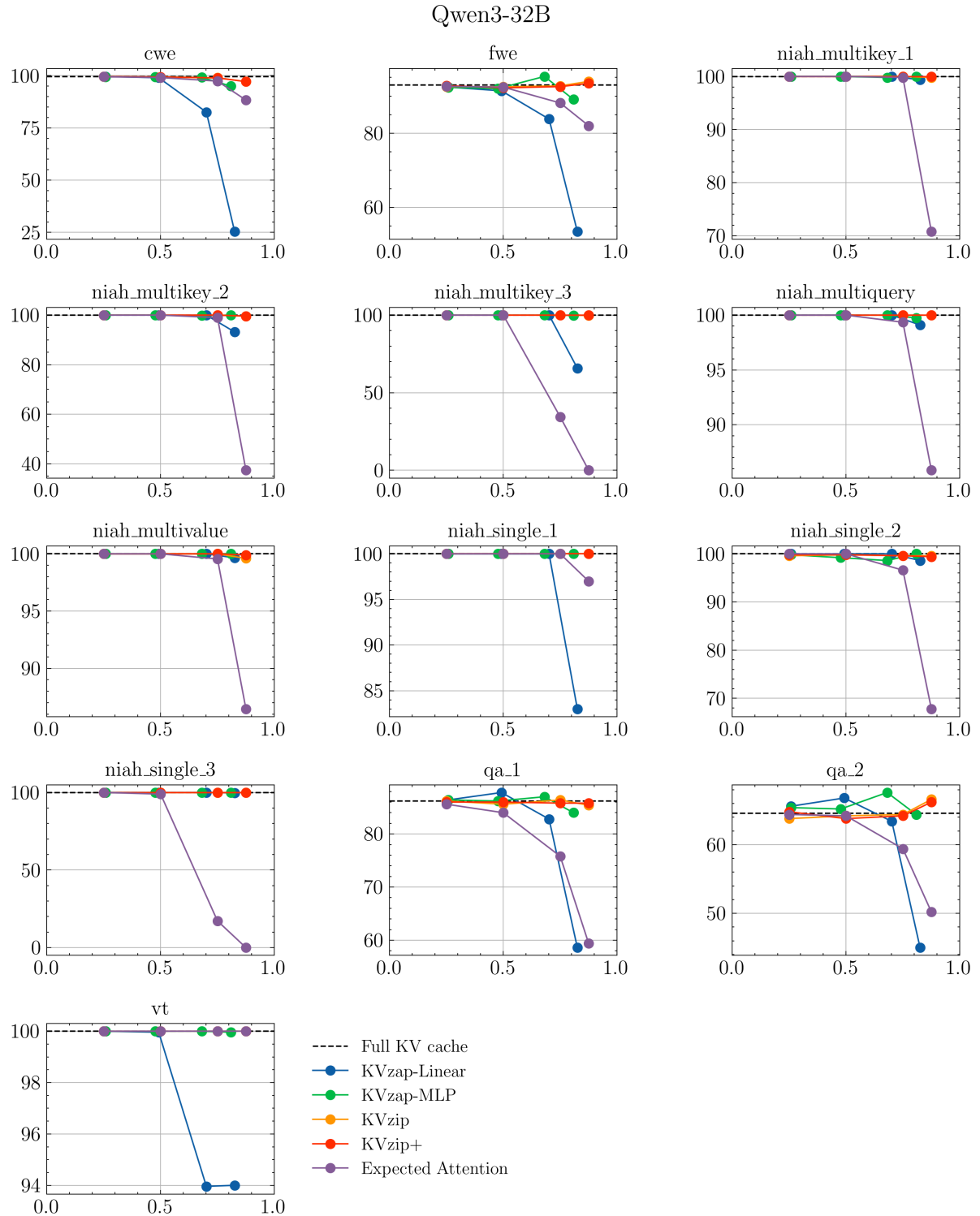


Figure 11 | RULER 4k results for Qwen3-32B on each of the 13 subsets

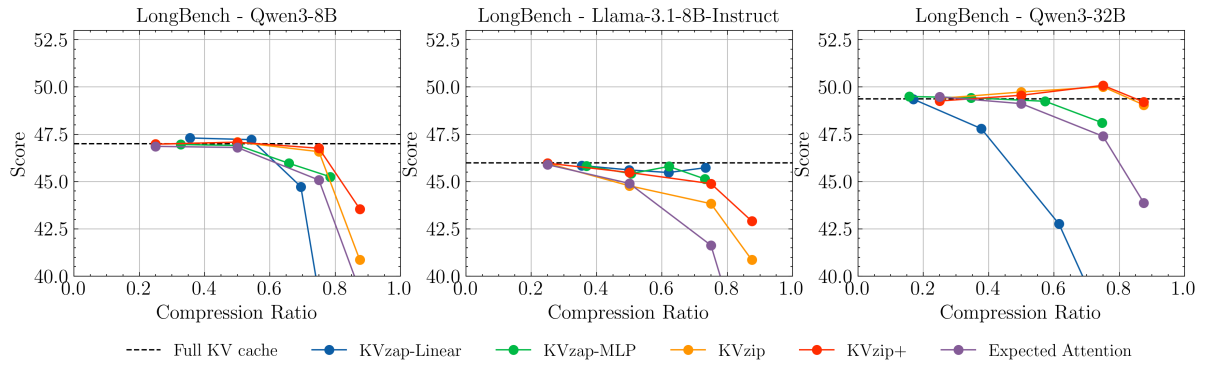


Figure 12 | **LongBench results** for Qwen3-8B (left), Llama-3.1-8B-Instruct (middle), and Qwen3-32B (right). Average score across 20/21 subsets, after excluding the TREC subset.

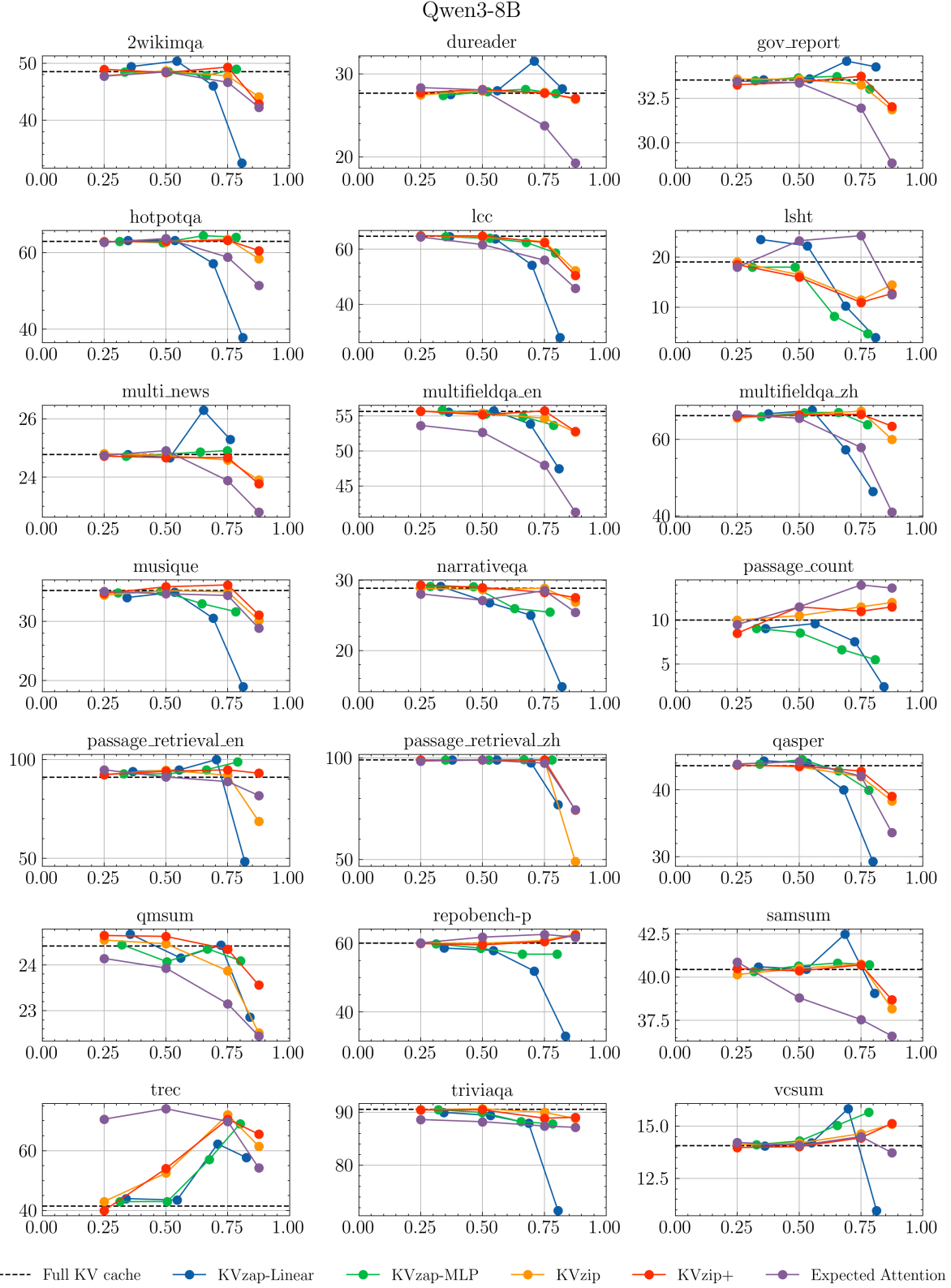


Figure 13 | LongBench results for Qwen3-8B on each of the 21 subsets

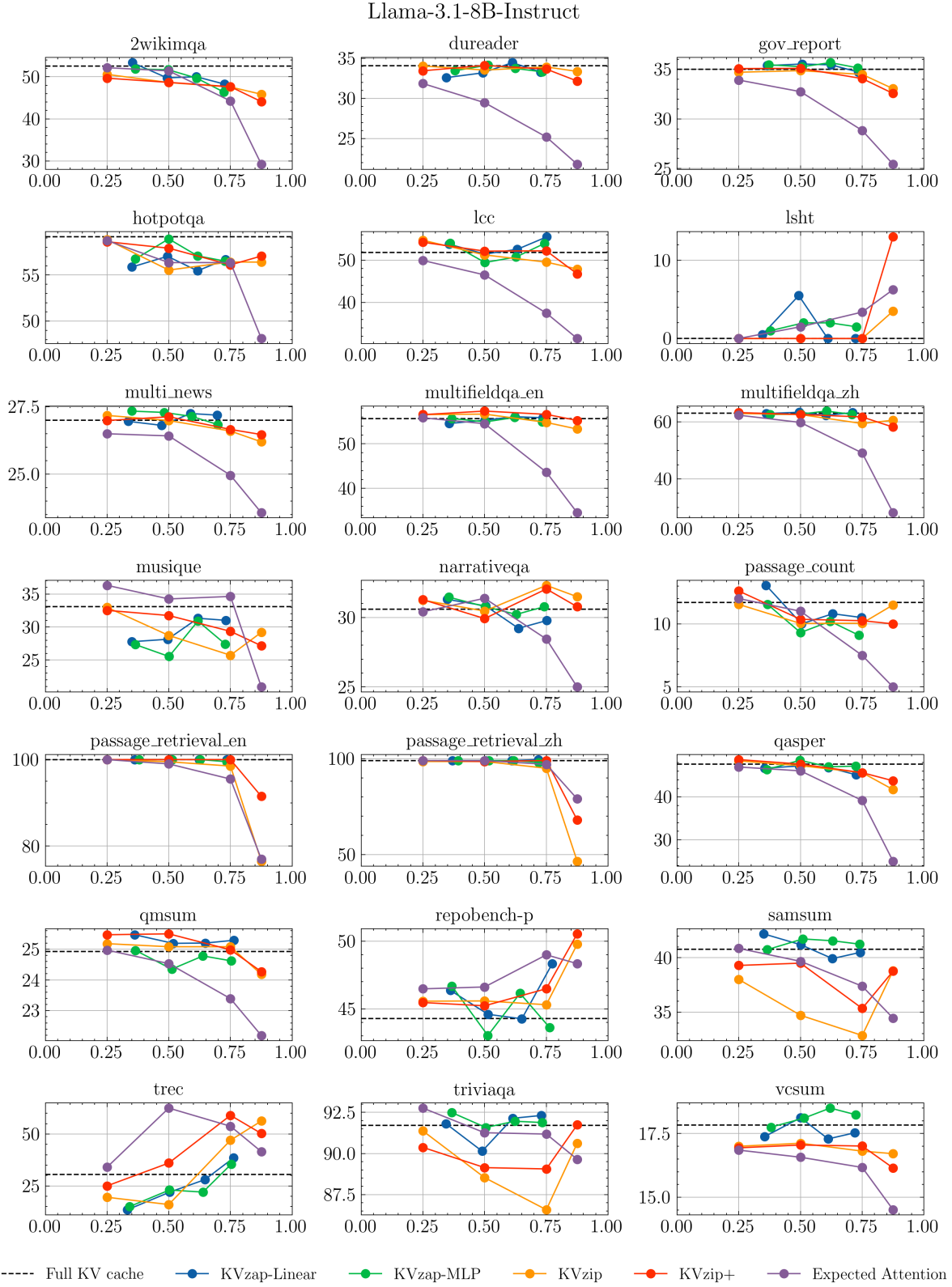


Figure 14 | LongBench results for Llama-3.1-8B-Instruct on each of the 21 subsets

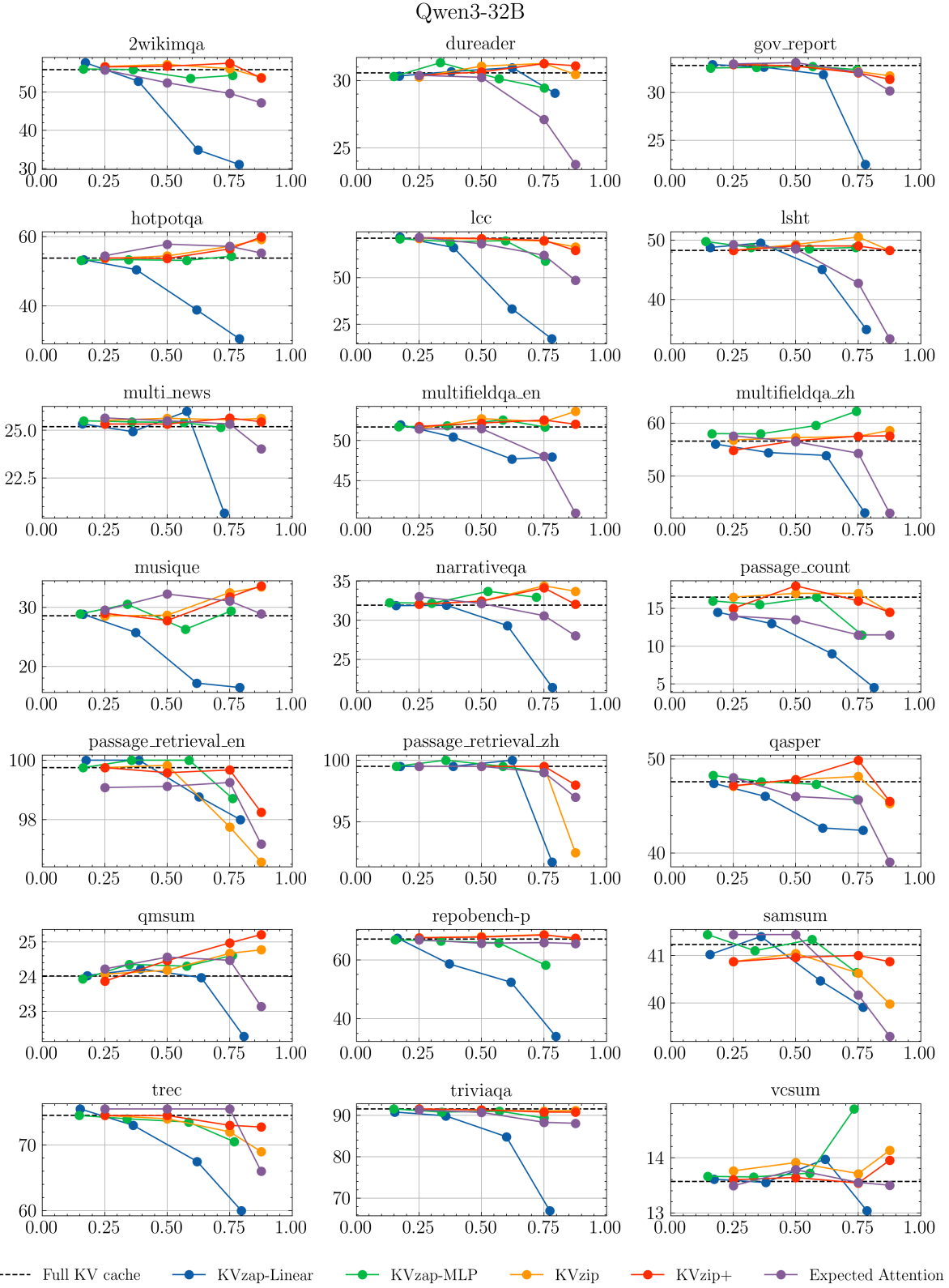


Figure 15 | LongBench results for Qwen3-32B on each of the 21 subsets